January - February 2020
ISSN: 0193 - 4120 Page No. 7698 - 7710

Experimental of Resting on Heat Transfer Performance of the Heat Pipe through Leading-Edge for Aircraft Anti-Icing Applications

Mr. P.Mohanraj, *Research Scholar, Department of Mechanical Engineering,Vels Institute of Science, Technology & Advanced Studies(VISTAS),Chennai-600117, Taminadu, India*

Dr. R.Sridhar, *Assistant Professor, Department of Mechanical Engineering,Vels Institute of Science, Technology & Advanced Studies(VISTAS),Chennai-600117, Taminadu, India. (Email: srisampangy@gmail.com)*

Article Info
Volume 82
Page Number: 7698 – 7710
Publication Issue:
January-February 2020

Article History
Article Received*: 18 May 2019*
Revised*: 14 July 2019*
Accepted*: 22 December 2019*
Publication*: 04 February 2020*

Abstract:
Recent research to increase the demand for energy efficiency in aircraft anti-icing technology and flight safety, investigating the performance of heat transfer using heat pipes is an efficient technique, which can transfer suitable solutions to congregate anti-icing and heat transfer requirements. Although past researches over a long time to be solved anti-icing system and still new innovative techniques demand for both military and civil aircraft. This examination investigates using Al2O3 nanofluids through a heat pipe on the superiority in the characteristics of the anti-icing system NACA 0012. Heat from 15 W to 170 W and the attack angle of -100 to 50 is used in experiments. The results of finding heat pipes using nanofluids are good anti-icing agents compared to other conventional methods and provide to achieve thermal equilibrium on the airfoil surface. Initially, temperature fluctuations were observed when AOA was not identical to 00 gradually and the positive angle had increased surface temperature. This experimental assessment related to icing avoids component failure during operation. The investigated results examined were the use of nanofluids in the heat pipe anti-icing system demonstrating potential techniques in the future.

Keywords: *Heat-pipe, Leading edge, Anti-icing, Temperature, Angle of attack.*

I. INTRODUCTION

Generally, airfoil consists of super-cooled droplets of high altitude failure of aviation components unfortunately affecting aerodynamic characteristics as a result of reduced drag and flight safety [1]. The formation of ice on the wings is a serious intimidation for failure and degradation to achieve better life competencies. The required efficient anti-icing method has been developed in the last few years. Bleed air anti-icing [2-3] and electro anti-icing [4-5] system are traditional method for anti-icing technologies due to the prosperity of energy [6]. These techniques are largely not used in Unmanned Aerial Vehicles (UAVs) because the use of air and electricity maintains the required working fluid temperatures. This fact looks forward to analyzing new anti-icing technologies. Heat pipe is an emerging technique to ensure that the heat source due to the capillarity pressure generate the porous wick under the evaporation-condensation closed cycles [7-12]. The porous wick has to rotate over a path with no extra power for transfer heat from the heat source. They results concluded using heat sink make advantages to demonstrate the high heat transfer coefficients, flexible travelling in excess of a long distance, energy savings and no additional requirements. Depending upon the needs, Loop Heat Pipes (LHPs) are proficient way to improve the heat

January - February 2020
ISSN: 0193 - 4120 Page No. 7698 - 7710

transfer and heat dissipation in anti-icing technology [13-16]. In future development of LHPs for commercial aircrafts anti-icing method is ensure that energy-saving value to over the other traditional anti-icing methods [17].

Loop Heat Pipes (LHP) as two-stage warmth move gadgets as shown in Figure 1 and consists of a condenser, evaporator, and reservoir and axis [18]. The characteristics of LHAP noted by "equivalent thermal conductivity" compared to metals more than one hundred times better. LHP is mainly used for effective thermal management for long distances compared to other traditional piping methods because of its function against gravity. Liquid pipes consist of condensers, evaporators, hydro-accumulators, liquid channels and steam lines. Many researchers review past studies of the operational characteristics of LHP thermal performance experimentally and numerically [19-21]. They use different methodologies to use heat pipes based on application as a result of the different operational characteristics of the LHP, which means it provides better reliability and operational flexibility of the LHPs. An aircraft safety at high altitudes is more important, as a result chemical stability, good heat transport properties, and beneficial axis infiltration are improved by using LHP. The wick is used only in the hydro-accumulator and relative to the evaporator and also the use of wall tubes made smoothly to transfer working fluid. The working principle of the LHP is evaporation due to the heat applied and the wick forming between the liquid-vapour interfaces. After evaporation vapor moves forward to the condenser, a Pressure force rise is developed because of the surface tension force. This process again uses the same surface tension as the liquid sent back to the evaporator. Evaporator has the main part as a compensation room and is connected to the evaporator as a secondary wick, located in places of the evaporator using a remote control system. The compensation chamber also functions as a reservoir and helps the circulation of external fluid by using Capillary Pumped Loops (CPL) for different versions of Liquid Heat Pipes (LHPs).

Many researchers using working fluid in heat pipe investigated for the aircraft anti-icing applications. The heat pipe design has prevented anti-icing by using heat emitted from air-oil coolers [22]. Furthermore, a new passive anti-icing system is proposed, as a result 3.8 kW of unused heat is removed from the hydraulic system using five types of LHPs [23]. During start-up conditions heat is produced for anti-icing systems. Gregori et al (2007) [24] examined anti-icing systems using five different types of fluid performances. They suggest water and alcohol are the best anti-icing agents compared to other traditional liquids. Ku et al. (2000) [25.26] reported, the effect of acceleration during start-up and working conditions of the LHP temperature distribution by using aluminum –ammonia as a result in steady state flow drastically affected vapor-liquid with the required temperature. Under steady conditions the effect of acceleration during start-up and operating temperature is expressed over long distances. Furthermore, they use a double combustion chamber to supply enough working fluid for the wick to be upgraded by an evaporator with different flight altitude conditions. The dual combustion chamber places both ends of the evaporator and investigates visualization of partial flow in the chamber and condenser. The result is derived relative to the vapor-liquid affected initially during the start-up operation of DCCLHPs [27]. Previous research investigations helped to solve various installation problems in anti-icing systems under different environmental conditions.

The schematic representation of Double Combustion Chamber Heat Pipe (DCCLHP) is shown in Fig. As designed by DCCLHP, CC is placed at both split ends of the evaporator and balances the liquid efficiently for the entire wick and remains wet underneath the different sloping conditions [33, 34]. This DCCLHP can solve more difficulties during the startup case and is able to start under a heat load to exceed the 50 W limits regardless of the tilt. Several studies examined the effects of acceleration on DCCLHP operating characteristics. The acceleration state of the LHP during the startup

January - February 2020
ISSN: 0193 - 4120 Page No. 7698 - 7710

case is easily adopted under stable conditions at lower temperatures. Subsequently, researchers at DCCLHP investigated depth experimentally and theoretically in future.

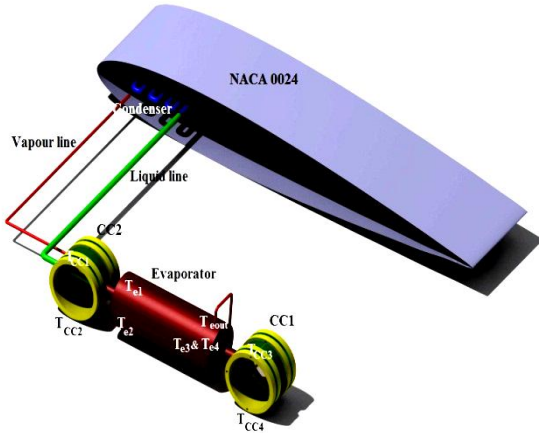

Fig.1. Structure of the Experimental DCCLHP

The current technology utilizes the development of nanofluids, which offer more benefits such as convective heat transfer with nanometer size, suspended metal components are inserted and increase the heat transfer coefficient by more than 20% compared to other conventional liquids and also reduce thermal resistance [28]. The heat pipe work fluids are classified based on the application of the heat transfer range at these temperatures, for mercury (523 - 923 K), Indium (2000 - 3000 K) and cryogenic temperatures (2-4K) using Helium and Nitrogen. Most researchers recommend ammonia (213-373K), water (298-573K), methanol (283-403K) and ethanol (273-403K) as working fluids for spacecraft and electronic cooling applications. Water working fluids have several limitations for heat transfer to heat pipes in anti-icing applications. The liquid nanofluid solution accommodates a thin film layer relative to the surface of the axis heat pipe and restrict the vapour bubbles capillarity strength and a blanket of steam creation has been avoided [29,30]. Li et al (2010) reported the investigated capillary pumped loop under the transient performance by using CuO-water nanofluid. As a result it was concluded the start-up time was reduced when increasing the concentration of nanoparticles [31]. So the maximum concentration of the nanofluid portion is coupled with a high amount of heat transfer. Chan et al (2015) [32] investigated the intentions of Al2O3 nanofluids related to heat pipe performance and identified the proportion of optimized nanofluids. LHP improves heat transfer performance by using nanofluids to apply optimal concentrations for better anti-icing special effects.

Previous literature reviews, the vast majority of experimental studies examined for anti-icing systems have been carried out at engine inlets using LHP characteristics. Likewise the small number of investigations reported regarding the use of anti-icing systems on wing LHP and those are formed the main objective of this study. This experiment investigates the characteristics of DCCLHP that experiences different angles and the use of the main aspects of Al2O3 fluid for anti-icing applications at the forefront of aircraft. Therefore, the main experiments carried out on DCCLHP using stainless steel and Al2O3 as working fluids with various concentrations were tested for three degrees of attack angle. Comparative and quantitative analyzes are carried out based on steady state experiments. This investigative study aims to understand DCCLHP's heat transfer performance for variable tendencies and also conduct nanofluids in anti-icing applications. In this connection, the DCCLHP experimental setups and conditions were explained based on the steady state conditions. The leading anti-icing effect on airplanes checks and enhances heat transfer performance under flight conditions and environmental conditions.

II. EXPERIMENTAL SETUP AND METHODS

Anti-icing experiments on leading aircraft were carried out for the FL-61 icing wind tunnel placed at the center of aerodynamics. The negative temperature was used based on the applications of anti-icing system. On the other hand experimental conditions on LHPs have certain limitations on aircraft for test always performed at the normal atmospheric temperatures. This type of wind tunnel can be operated by flight and environmental conditions such as atmospheric temperature and air transfer speed. Cross sectional area of the wind

January - February 2020
ISSN: 0193 - 4120 Page No. 7698 - 7710

tunnel is 0.5x0.4x0.3m. The DCCLHP representation has been designed and built for the current investigation as the layout settings shown in Figure 1. This DCCLHP works with parts such as LHP, condenser, liquid channel, steam channel, evaporator and space and data acquisition system. Nickel is used to make wick and steel is also used for evaporator, condenser and liquid vapor lines. Apart from the above components, the double compensation space is distinguished from what is referred to as CC1 and CC2. DCCLHP of the designed specifications are presented in table 1.

Table 1 Geometric specifications of DCCLHP

Component	Description	Parameter
Evaporator	O.D x I.D x L	52x45x120 mm
Vapor groove	Length x Width , Number	1x1 mm, 11
Vapor/liquid line	O.D x I.D x L	3x2x500 mm
Condenser	O.D x I.D x L	3x2x500 mm
wick	Porous radius	1.2 µm
CC1	Volume	59.5 ml
CC2	Volume	59.5 ml

In experimental setup, the thin film heater is attached directly to the symmetrical case evaporator for observing heat load and engages the alternate AC current forced on the heater. This test section enhances the three main parts of the DCCLHP system such as tunnel, heating system and data acquisition system. The various functional and sub components are entirely shows in graphical representation Figure 2. In a data acquisition system recognized the temperature over a surface by placing various positions of thermo couples. The system named by Agilent 34972A and records the every 20 seconds time interval of temperature distributions.

The transport lines utilized the thermal insulation coating for reduces the heat losses to the atmosphere. Although, the thermal insulation of an inner layer possessed by nano coating, which was fabricated form the ceramic ball and water-based chemical as polyacrylic and for the thermal conductivity 0.00012 W/(m-K). The experimental test results found under the steady state procedure is followed by homogeneously. Primarily the nanofluid used charge the LHP and places a LHP to horizontal orientation at same level of component were appropriated. Further, air velocities set to the wind tunnel and enhance the heat load to the evaporator. However, before the start-up condition to pass the time for when the temperature reached the stationary values or oscillating in the temperatures differences. The same procedure was followed until end of the experiments for various heat loads and different fuel concentrations.

In order to minimized the experimental error due to the non-uniform flow near to wind wall when the wind is fixed as more flexible around the wing. Therefore the middle section only used to measure the heat transfer performance of LHP and condenser also located near to LHP as a three dimensional figure as shown in Figure 3.

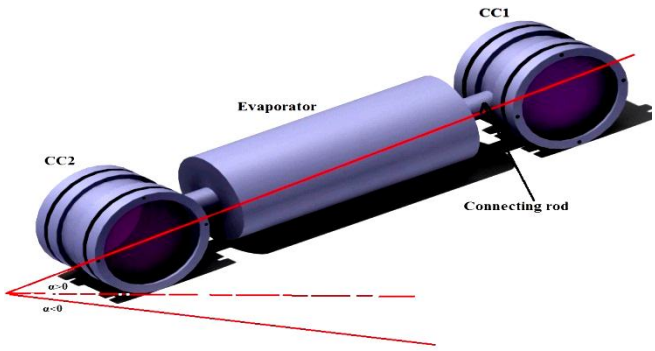

Fig.2. Structures of the evaporator and CCs.

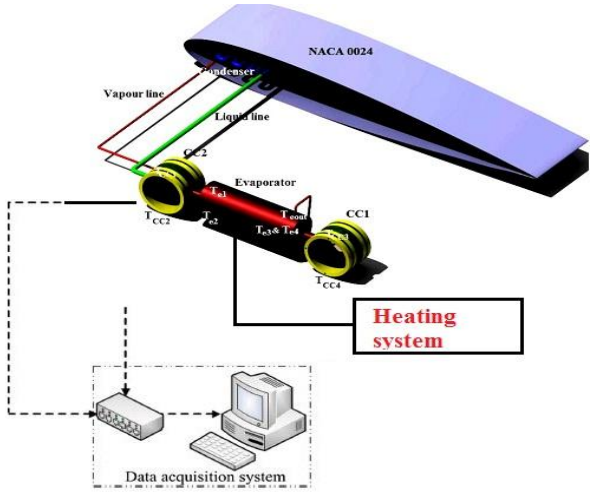

Fig.3. Schematic representation of the experimental setup

For the condenser, to ensure all the warmth of the vapour working liquid can be moved to the flying

January - February 2020
ISSN: 0193 - 4120 Page No. 7698 - 7710

machine skin, the protection of the tubing must be made to lessen the warmth move between the vapour and the air inside the wing. Layer 1 is warm protection nano-covering, which is produced using the clay ball and the polyacrylic water-based synthetic, with the warm conductivity 0.0012 W/ (m2K). Layer 2 is elastic with the thickness of 3 mm. There is also a warm silica gel that is filled between the skin of the plane and Layer 2, thereby reducing contact warm obstruction and increasing warm conduction. On the skin of the aircraft, seven T-type thermocouples were installed together with harmony pads to record surface temperatures. Point 6 is the point of stagnation. The separation between each thermocouple is 20 mm along the shallow harmony path.

A. Experimental cases

In this investigation of various process parameters for anti-icing applications, it seems under the usual aircraft of operating conditions. For Inclination refers as a default rolling angle 100 used in the aircraft and total angle covers ±200 to 00. According to the usual aircraft conditions condenser is often placed above and below the evaporator within direction of gravity as an angle 200 and -200 for accepted states. So far the 00 represents the orientation of LHP on horizontal positions, which means components are all in same level. The compensation chamber placed depending upon the jack mechanisms of detailed designs are shown in Figure 4. The jack mechanism of section 1 and section 2 both are designed with a thread form, which can be adjusted that they require length. Consequently, the condenser and evaporator adjusted to the direction of gravity and achieved angle inclinations for the required length by using jack mechanisms. The working fluids have some limitations in thermophysical properties are mutually restrained the heat transfer performance and startup process of LHP.

However, the various mixtures contribute effectively succeed to superior characteristics by use of every component, as a result achieved relatively the better heat transfer performance and startup. The lower heat load describe the Al2O3-water nanofluid behaves smooth startup than water due to the mixture decreases the startup heat load and operating temperatures of LHPs, while Al2O3 has easy for vaporization and boiling point. Similarly, at high load increasing water content to Al2O3 might be increased the energy in terms of high heat transfer over a long distances due to latent heat vaporization and enhance more surface tensions.

Besides, the characteristic stage change hindrance of the Al2O3 to be vaporized more rapidly than water and the vapor weight is higher than the immersion weight of water at a similar temperature, which result in limitation of vaporization of water and that's just the beginning water maintenance in fluid stage. The condenser made of water condenses quickly than the Al2O3 and it can be easily send back through the evaporator. Thus the way to receive the waste heat from the evaporator and also liquid could be circulate from the condenser that heat transfer has maintained between the hot and cold atmospheric conditions. Normally, the aircraft icing reached at an altitude of 6000m -8000m, when the estimation of ambient temperatures presents -200C. In this study, corresponding volume concentrations of Al2O3 mixed with water as 40%, 60%, 805 and 100% respectively. The preparation has followed by the standard procedures as result water could distill and degassed before the mixing with Al2O3.

Moreover, investigate heat transfer performance for the effect of heat load and thermal resistance on LHP leading aircraft anti-icing applications. The heat flux, density and other appropriate parameters are designed under the real aircraft leading edge anti-icing methods. In a steady state operation 25 % concentration cannot achieve the recommended results. The limitations proved the heat load lies between the 100W to 300 W, increments for every step 20W. This investigation designed the steady state parameters are listed in the table 2. This type of angle variation sequence is specifically used to validate the ability of the LHP to handle the time for the rolling maneuver.

January - February 2020
ISSN: 0193 - 4120 Page No. 7698 - 7710

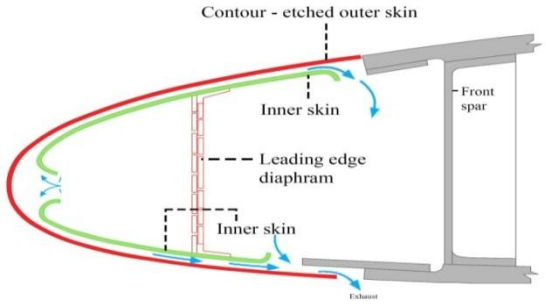

Fig.4. NACA 0024 Leading edge anti-icing significance

B. Data reduction and uncertainty analysis

Thermal resistance (R) on DCCLHP expressed as

$$R = \frac{\Delta T}{Q}$$

$$R = \frac{T_e - T_{cond}}{Q}$$

$$T_e = T_{e\_Out}$$

$$T_{cond} = \frac{1}{2}(T_{cond\_in} + T_{cond\_out})$$

Where Te- Evaporator temperature, T_{cond} - Condenser temperature, T_{cond_out} -Outlet temperature of the condenser, and T_{cond_in} - Condenser temperature at inlet and Q-heat load. The least temperature was used in the test 20.50C and for the uncertainty temperature is 2.46 %. The thermocouples accuracy is chosen default value ±0.5. This experimental has utilized the maximum current 0.7A and 100A respectively and also the voltage in the supply system is 1.5V. Similarly, the uncertainty analysis for current and voltage are 6.43% and 3.75%, and uncertainty for heat load is 7.4%, thermal resistance R is 7.84%.

III. RESULTS AND DISCUSSION

A. Startup process

The LHP startup process is an important criterion for aircraft leading edge anti-icing applications. The beginning up time is from the minute when the warming force is joined on the evaporator to when the condenser channel temperature starts to rise. The sudden climb of the condenser inlet temperature and the final dependence on the temperature of the entire framework means the startup achievement of the LHP. For shortest time represent the LHP has aimed to start their work for anti-icing systems. While the startup process meet with dynamic process as circulating the working fluid and phase changes between the condenser and evaporator. The experiments were conducted for the AOA 00, ±50 and 100, heating power 100 W, wind velocity 12m/s as a results analyzed the effect of nanofluid on LHP anti-icing applications.

During the startup conditions, the evaporator outlet rises in all respects gradually at the first or two minutes however very quick during the following couple of minutes. Although the heat was observed from the heat source to the Al2O3- water working fluid by using conductive heat transfer method. At the beginning stage evaporator connected with the heat source and whole system of temperature equally treated as environmental temperature. At some point in time to evaporation, the temperature of the shell and working fluid wants to increase the room temperature into evaporator temperature , those process named by preheat period. This stages of preheat, generated few amount of vapour in evaporator and created the vapour pressure is low.

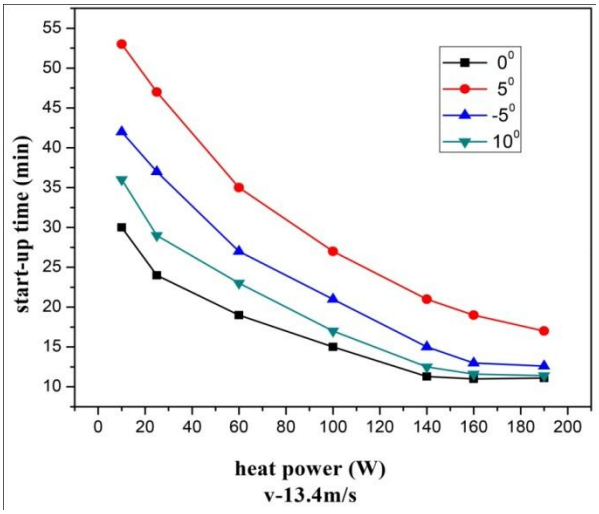

Fig.5. Start-up time with influence of the AOA

The preheat period of time generation vapour gradually increased slightly move to the vapour line and passed away from the working fluid. Similarly, the condenser initially maintain the low temperature remains constant and further increases rapidly for begins to start. From the Fig 5, that indicates the vapour responses up to 10 minutes for relieving the

January - February 2020
ISSN: 0193 - 4120 Page No. 7698 - 7710

working fluid absent of the vapour line and pushed from evaporator to condenser. Thus the main functions for sustains of good anti-icing possessions, that the anti-icing DCCLHP must be switched on before the aircraft encountered in to super-cooled droplets. Based on the applications different designs are still needed for LHP anti-icing system.

Furthermore, observations are recorded from the experimental analysis of DCCLHP startup process. As a results concluded for high temperatures are observed by various sections such as condenser inlet, evaporator outlet and liquid line inlet of the DCCLHP system where the AOA required 00 and ±50. The variations in AOA 50 and 100 is wider than the -50 AOA, due to the existing angles are changing the flow characteristics of a vapour and working fluid in the evaporator. At the time primary wicks are accumulated the vapour channel of the evaporator shell, when the heat source always attached to the evaporator. After the flow passes away from the evaporator, suddenly rise in temperature to the evaporator outlet. It ought to be seen that the width of the interfacing funnel is bigger than that of the evaporator outlet, as is appeared in Fig. 6

The flow resistance comparatively low to the evaporator and increase the vapour mass owing to the flow characteristics, easy to vapour flows through CC in higher altitude as a result increasing the temperature of the CC and reduce the temperature in evaporator outlet. The CC becomes stable when utilizes the both vapour and liquid, during the vapour flow out of the evaporator continue to finish their startup process and enhance the high temperature of the evaporator outlet. Therefore the temperature of the higher CC is larger than that of lower CC for the anti-icing techniques on leading edge aircraft.

Moreover, the physical phenomena attributed instability of vapour liquid in CCs might be tribute the temperature fluctuations of DCCLHP system. At the point when the warmth burden is appended on the evaporator, there will be vapor and fluid existing in the CCs with the impact of the warmth spill from the evaporator. The temperature distributions for AOA 50, -50 and 100 on CC1 is 91.1, 75.3, and 94.7 and CC2 temperature is 66.2, 75.6 and 50.40 C. From the results clearly proved the temperature of CC1 is higher than the CC2 due the vapour line accumulated the latent heat to the higher CC. The AOA 50 and 100 observed temperature fluctuations at near the liquid line working fluid. This liquid line always closely related to CC1 for easily affected by the vapour flow and thermal conduction from the bayonet. Furthermore, the startup time of shortest duration indicates anti-icing systems can works, as a results effect of time and distance influences the startup cases.

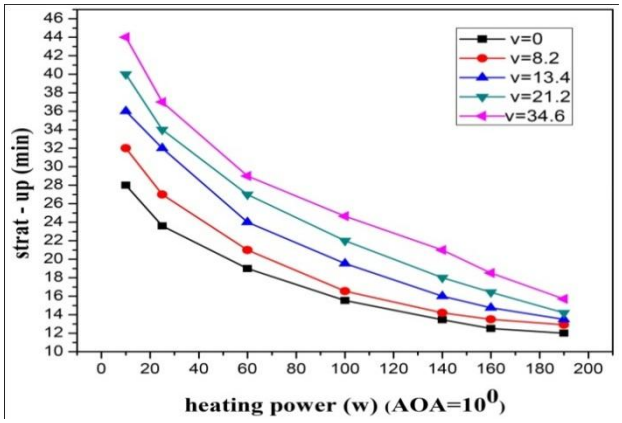

Fig.6. Effect of velocity on the start-up time

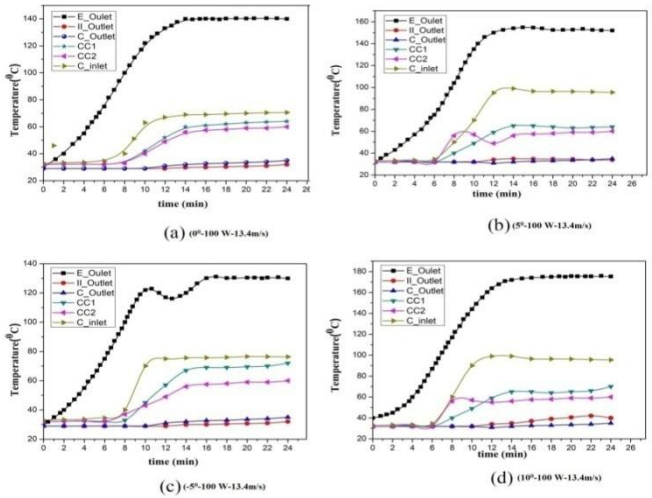

Fig.7. Start-up process of the DCCLHP anti-icing system.

The impact of the AOA on the beginning up time demonstrated from the outcomes that the beginning up time with AOA 0 is the briefest. The greatest beginning up time contrast with Q = 10W is 17 min, and this worth reductions to 3.2 min when the warming force is expanded to 180 W. Along these

January - February 2020
ISSN: 0193 - 4120 Page No. 7698 - 7710

lines, when the warming force is low, the impact of AOA on the beginning up time is more prominent than that when warmth power is high. The various angles of attacks cause different distributions in liquid and vapour line. When the low heat power obtained slower vapour generation. A large portion of the heat is utilized to raise the temperature of the working liquid from the room temperature to the dissipation temperature. However, the mass vapour and flow velocities both are easily affected by whole system of a LHP. The angle of attack is not 00, the vapour will transfer into CC which is higher in the arrangement. The similar deals with the temperature fluctuation and decreases the vapour mass pour into the condenser. It was increases the start-up time seeing as vapour flow through condenser and need to finish the start-up process by working fluid push away from the condenser.

The positive AOA preferred a liquid line is wider than the vapour line and the working fluid sends back to the evaporator due the gravity, since the start-up time will be increased to longer as shows in Fig 7. Also the negative AOA stated that the liquid line is lower than the vapour line and gravity allowed flow back of the working fluid. Due to the buoyancy effect, the vapour accumulated right side of the evaporator and more liquid gathered to left side of the evaporator which one of the CC1 is higher. It may delay the start-up process by reason of buoyancy effect hold back the vapour flowing out from the evaporator.

Besides, the air velocity plays an important role for start-up process as a result shown in Fig 6. The effect of air velocity on start-up time for AOA 100 as where the heating power increases the start-up time becomes shorter. It is an important evident for observe the high heat power resumes the heat from the heater to working fluid more fastly and easily vapour can be generated in the evaporator. The vapour pressure also increased in the evaporator and so far shortening times are required to move a vapour into vapour line and then transferred into the condenser as noticed for obtain shorter start-up time. And some start-up cases attributed higher velocity, heat power and long start-up time due to when increases the air velocity will formatted to gets air stronger between the aircraft skins, as a temperature was reduced where the flow passed out from the condenser. However, working fluids are flow back to the evaporator, since the vapour temperature and too evaporator temperature was decreased. As a result start-up time gets longer due to the decreasing state of evaporator temperature. In order to reduce the drawbacks and maintain the successful start-up needs some pressure and required vapour mass.

B. Thermal Resistance

The thermal resistance at DCCLHP reflects the intensity of the working fluid heat transfer characteristics and thermo physical properties. The expansion of heat source, the heat opposition of the framework gets lower rapidly from the start and afterward will in general be steady when the warming force is higher than 100 W. As a result of reporting, the system condenser cannot be activated with under 100W.The thermal conductance area varied due to the fluctuation in heat power from the heat source of the LHP. This activating condenser and stable thermal conductance area needs high power from the evaporator in the LHP system. The experiments shows and obtained low thermal resistance of LHP for AOA 00 and therefore the thermal resistance have increased when AOA noticed higher. Above mentioned thermal resistance equation of the LHP describes, the low thermal resistance causes the flexible LHP system efficiently by the reason of evaporator temperature is closer to the condenser temperature. The graphical curve Fig 8 tends to increase heat load with corresponding effect of thermal resistance, which results are obtained similar to the past researchers. The thermal resistances are decreased progressively for the various mixtures 25% and 50% as results 0.44 to 0.190 C/W and 0.25 to 0.17 C/W correspondingly. It is noticed from the graphical plots, the both values are lies between 100W to 270 W. Unfortunately the thermal resistance curves are slightly increased at near the 260 W. However the lower heat loads, expanding heat burden

January - February 2020
ISSN: 0193 - 4120 Page No. 7698 - 7710

prompts more vapor invention and a bigger successful heat source moves territory in the condenser, which result in the reduction of the condenser heat opposition. Therefore 75% nanofluid working fluid from the mixture sees that the results of the thermal resistance are initially reduced when increasing the heat load from 100 W to 300 W. The 75% performance concentration on the LHP decreases at the maximum endpoint of 260 W. For the unadulterated Al2O3, the variation pattern of heat obstruction as a component of heat burden was like the 75% gathering, then again, actually the basic point pushed ahead to 200 W. It is shown the exhibition of unadulterated Al2O3-water begins to fall apart at 200 W. The output results described in low concentrations of Al2O3-water nanofluids lead to work at high heat loads with sufficient heat transfer capability.

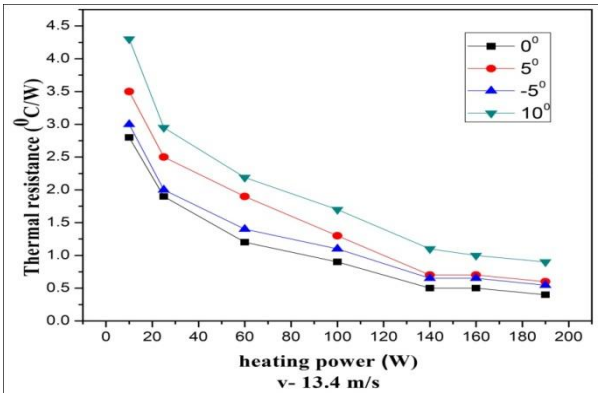

Fig.8. Thermal resistance of the DCCLHP

The thermal resistivity of the mix 25%, 50%, 75% and 100% is different in the LHP for the maximum heat load found in the 25% mixture which is greater than the other mixtures, but the maximum heat load found is less than 290W. Because of the following some physical characteristics are perceived high latent heat vaporization, maximum boiling point of water, high specific heat, and recover the poor vapour generation and lower heat load observed large thermal resistance on LHP. As watched, the heat opposition with unadulterated Al2O3 conquered that with 80% grouping of blend at 280 W, and turned into the most extreme at 290 W. This phenomenon indicates to characters of nanofluids such as phase-change hang-up theory and fewer concentrations could be found high heat transfer capability for higher heat load from the LHP.

As indicated by the innate physical properties of Al2O3-water blend, with lower breaking point forces stage change hindrance on the vanishing of the water with a higher breaking point. At the same temperature Al2O3 evaporates faster than water and vapor pressure is also shown to be higher than water saturation pressure during the phase change occurs. This phase changes occupies the more water retention in liquid phase. For the opposite process to occur in the condenser, the water condenses more easily than Al2O3 and is transferred easily to the evaporator and forms a wet axis. This trademark clarifies the LHP accused of a blend with more proportion of water acquires the littler warm protections. The above persistent state results resolves there exist evident potential to improve the exhibition of the LHP by utilizing Al2O3-water a blend as far as accomplishing lower working temperature and thermal resistance.

C. Operating temperature of the LHP

The lower heat load 100W on LHP as results obtained for a maximum and minimum temperature is 1200C and 152.1 0C respectively. As seen that heat load 260W of all the temperatures relative to each together. In order to increases the heat load 300W, among the four concentrations of temperature increased over again. Thus for the results observed Al2O3 without water mixtures achieved maximum temperature 197.540C for 25% concentration and 75% mixtures attain the lowest temperature 167.50C respectively. It ensures that water is always closely related to the Al2O3 for the facts of latent heat vaporization, specific heat and boiling point. However, the Al2O3 working fluid compared with the other conventional fluids easily vaporized at lower heat loads with yielding lower operating temperatures. Be that as it may, because of the lower inactive heat of vaporization and surface strain of Al2O3, the lacking warmth move capacity and even halfway dry out of the wick show up for the blend with a bigger extent of Al2O3 nanofluid at higher

January - February 2020
ISSN: 0193 - 4120 Page No. 7698 - 7710

thermal loads. During the dry out conditions, the wick couldn't be held totally wet under this condition and Dry out is portrayed by the development of vapor rises on the engrossing faces of the entire wick. In the event that all out weight misfortunes in the framework surpass the capillarity limit of the fluid furthest reaches that the wick can give, the condensate fluid is never again ready to come to the evaporator, dry-out of the wick will happen. This wick conditions found lower resistance from the evaporator to CCs under the vapour flow passages. At the time of loop operation has suddenly increases the operating temperature of the lower concentration mixtures at 300 W for enhance the heat transfer performance.

As Fig 9 is shown that of operating temperature versus to the corresponds heat load among the four proportions of mixtures. This warmth load reliance of the working temperature is extremely uncommon to the uninvolved LHP framework, which is identified with the measure of parasitic warmth spillage from the evaporator to the CC, fluid stock inside the CC and cooling the limit of the approaching condensate from the condenser. The evaporator temperature (Te) of the LHP has characterized by different aspects such as heat load, dimension of LHP, types of working fluid, source of cold temperature respectively. From the graphical curve clearly indicates the operating temperatures for 25% and 50% with a heat load from 100W-300W gradually slow to increase, which can be lies between 141.30-2020 C and 134.30- 185.40 C respectively. But specifically the operating temperature for 75% and 100% of mixtures of heat load increased at above 160W. In this case, due to the lower heat load and steam mass flow rate indicates the full liquid that is occupied in the condenser and CCs to some extent is filled with liquid. Further, the condenser needs large phase-change area due to the increasing heat load and flow rate of vapour content.

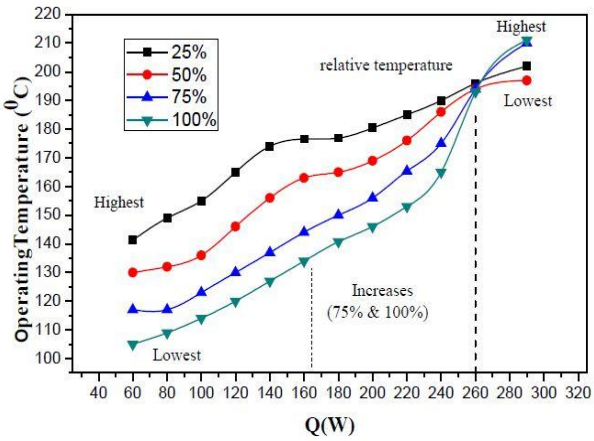

Fig.9. Operating temperature vs. heat load with different concentrations of Mixtures.

The phase changes in the condenser adopted the vapour drives liquid from the condenser to CC. As a result the heat capacity increases inside the CC and thus strongly affected the heat leakage, and causing small variations in temperature to display. In any case, because of the lower idle warmth of vaporization and surface pressure of Al2O3, the deficient warmth move capacity and even incompletely dry out of the wick show up for the blend with bigger extent of Al2O3 at higher heat loads, consequently the working temperature gives a more extreme increment further expanding the heat load.

D. Surface Temperature

The effect of AOA and heating power on the leading edge surface are shows in Fig 10. From the observation the surface temperature relative to the skin surface, when the heat power increased the temperature was raises gradually. This temperature rises due to the latent heat vaporization, conduction, convection and sensible heat of the working fluid. The system of design consists of three phases such as vapour and liquid line and combination of the vapour liquid line. However, the convection rate decreases as a result others determination increases the temperature raising. Generally starting point of the condenser has to obtained the vapour is high with the temperature and pressure. While the cooling air causes on the upper surfaces skin to the vapour change into stagnation point due to exists of vapour

January - February 2020
ISSN: 0193 - 4120 Page No. 7698 - 7710

and liquid. Then the saturation point in a two-phase flow continuously the working fluid transfer the heat into the leading edge skins, where the vapour is fully condensed to liquid and the fluid enter into the super-cooled state. Besides, the graph shows some distances have increased from the stagnation point as a result convection starts to decreases by the reason of the temperature initially closes to the condenser inlet when the vapor pressure and temperature is very high on the aircraft leading edge. Whenever the airflows enters into the stagnation state, those velocities are decreases to 0 when the temperature gets lower at the testing points number 6 due to existences of skins.

This is an effect of boundary layer thickness at the stagnation point, which states that convective heat transfer significantly high. It is an important evident for decreases the temperature due to the effect of high convection. However, the testing point 7 gets slightly higher than the point 6 as a concluded certain stage after the stagnation point the cooling effect strongly affected the convection. The surfaces temperature for positive Angle of Attack 50 obtains higher compared with the negative AOA. This can be describing the successful start-up process. Further, the vapour easily accumulated in the vapour channel near to the CC1 and the flow out convert into condenser fastly means the evaporator placed in the higher position with positive angle of attack. On the other hand for negative AOA of flow out process gets more difficulty due to the working fluid highly accumulated in the evaporator as a result the condenser inlet temperature decreased.

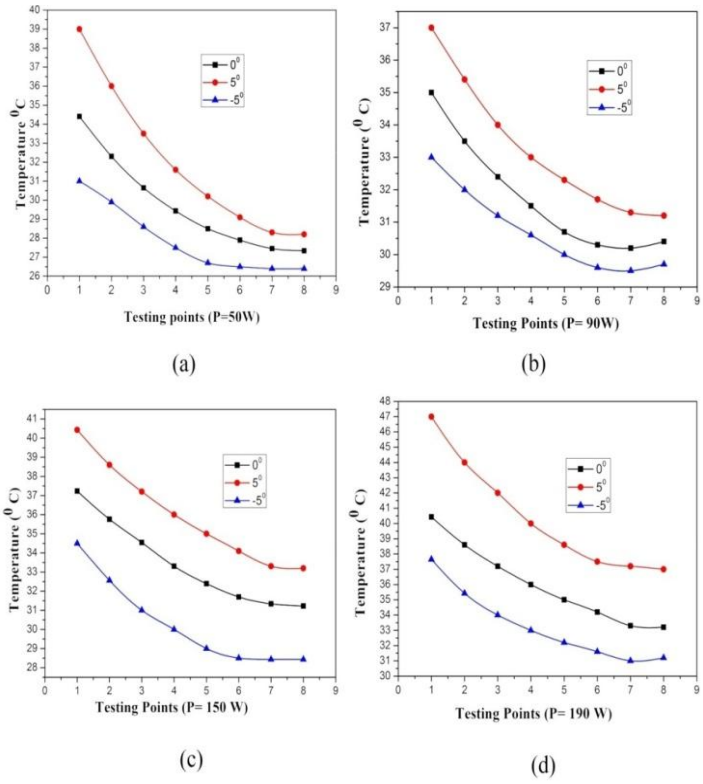

Fig.10. leading edge Surface temperature for different heating power and AOAs.

IV. CONCLUSION

In this examination, the experimental process of the DCCLHP with the representation of CCs was done. The fundamental aftereffects of this examination can be abridged as pursues:

To successfully utilize the better thermophysical transportation characteristics of water and keep away from its solidifying issue under negative temperature conditions, the Al2O3-water blend was in use as the working liquid in the structured DCCLHP for flying machine hostile to icing. It gives another plan to the acknowledgement of applying DCCLHPs to airbus machine anti-icing.

The positive AOA can build the surface temperature, because of which the anti- icing impact could likewise be upgraded. Therefore, the influencing of AOA can causes the temperature oscillations of an entire DCCLHP setup and also could affect the operating temperatures of DCCLHP.

So it is proposed that the evaporator outlet ought to be placed in a higher altitude, when AOA is sure that if the flight bearing and the pivot of the evaporator is

January - February 2020
ISSN: 0193 - 4120 Page No. 7698 - 7710

analogous

DCCLHP can startup effectively with thermal loads from 5W to 190 W. Because of the time required to start, DCCLHP hostile to the hardening frame must be turned on a few minutes before the airship experiences fog.

The surface temperature of the leading edge increments with the expansion of the heat control on top of the evaporator.

From the steady state results clearly indicates lower operating temperature and lower thermal resistances are obtained for a concentrations 50% mixture , it enhance to the better heat transfer characteristics during the steady state.

V. REFERENCES

1. S. Chang, W. Yu, M. Song, M. Leng, Q. Shi,(2019) "Investigation on wavy characteristics of shear-driven water film using the planar laser induced fluorescence method", Int. J. Multiphase Flow .
2. F. Saeed, (2008) "Numerical simulation of surface heat transfer from an array of hot-air jets", J. Aircr. 42 (2) 700–714.
3. W. Dong, J. Zhu, M. Zheng, Y. Chen, (2015) "Thermal analysis and testing of non-rotating cone with hot-air anti-icing system", J. Propul. Power 31 (3), 1–8.
4. L. Bennani, P. Villedieu, M. Salaun (2013), "Two dimensional model of an electro thermal ice protection system", AIAA Paper, No. 2013-2936.
5. S. Chang, Y. Hou, X. Yuan, (2007) "Influence of periodic electro-heating pulse on deicing surface temperature", J. Aerosp. Power 22 (8), 1247–1251.
6. W.G. Anderson, P. Chow, (1995) "Loop heat pipes for anti-icing of gas turbine inlets", J. Clean. Prod. 3 (4), 243–244.
7. M. Mitomi, H. Nagano, (2014) "Long-distance loop heat pipe for effective utilization of energy", Int. J. Heat Mass Transfer 77 (4), 777–784.
8. J. Ku, "Operating characteristics of loop heat pipes, SAE Technical Paper", 1999- 01-2007, 1999.
9. Y.F. Maydanik, (2005) "Loop heat pipes", Appl. Therm. Eng. 25, 635–657.
10. X. Zhang, X. Zhao, J. Xu, X. Yu, (2013) "Characterization of a solar photovoltaic/loop heat-pipe heat pump water heating system", Appl. Energy 102 1229–1245.
11. X. Zhang, X. Zhao, J. Shen, J. Xu, X. Yu, (2014) "Dynamic performance of a novel solar photovoltaic/loop-heat-pipe heat pump system", Appl. Energy 114 335– 352.
12. X. Zhang, J. Shen, P. Xu, X. Zhao, Y. Xu, (2014) "Socio-economic performance of a novel solar photovoltaic/loop-heat-pipe heat pump water heating system in three different climatic regions", Appl. Energy 135 , 20–34.
13. Q. Su, S. Chang, Y. Zhao, H. Zheng, C. Dang, (2018) "A review of loop heat pipes for aircraft anti-icing applications", Appl. Therm. Eng. 130 , 528–540.
14. A.L. Phillips, K.L. Wert, (2000) "Loop heat pipe anti icing system development program summary, SAE Technical Paper", 2000-01-2493,
15. A.L. Phillips, N.J. Gernert, (1998) "Passive aircraft anti icing system using waste heat, SAE Technical Paper", 981-542.
16. C. Gregori, D. Mishkinis, P. Prado, A. Torres, R. Pérez, (2007)" Loop heat pipe technology for aircraft anti-icing applications". SAE Technical Paper, 2007-01-3312.
17. W.G. Anderson, P. Chow, (1995) "Loop heat pipes for anti-icing of gas turbine inlets", J. Clean. Prod. 3 (4), 243–244.
18. Edition F, Reay D, McGlen R, Kew P. (2013) Heat pipes: Theory, design and applications. Butterworth-Heinemann.
19. Yuming Chen, Manfred Groll, Rainer Mertz, Yu.F. Maydanik, S.V. Vershinin, (2005) "Steady-state and transient performance of a miniature loop heat pipe", Int. J.Therm. Sci. 45 (11) 1084–1090.
20. L. Bai, G. Lin, H. Zhang, D. Wen, (2014) "Effect of evaporator tilt on the operating temperature of a loop heat pipe without a secondary wick, Int. J. Heat Mass Transfer 77 (4) ,600–603.
21. S.V. Vershinin, Yu.F. Maydanik, (2007) "Investigation of pulsations of the operating temperature in a miniature loop heat pipe," Int. J. Heat Mass Transfer 50 (25) , 5232–5240.
22. W.G. Anderson, P. Chow, (1995) "Loop heat pipes for anti-icing of gas turbine inlets, in: Proceedings of the IX International Heat Pipe

January - February 2020
ISSN: 0193 - 4120 Page No. 7698 - 7710

Conference “, New Mexico, USA, May.
23. A.L. (Fred) Phillips, Kevin L (2000). “Wert, Loop heat pipe anti icing system development program summary”, in: 30th International Conference on Environmental Systems. Toulouse, France, July 10–13. Paper No. 01-2493.
24. Carmen Gregori, DonatasMishkinis, Paula Prado, Alejandro Torres, Ramón Pérez (2007), Loop Heat Pipe Technology for Aircraft Anti-Icing Applications, SAE Paper, No. 2007-01-3312.
25. J. Ku, L. Ottenstein, T. Kaya, et al., (2000) “Testing of a Loop Heat Pipe Subjected to Variable Accelerating Forces”, Part 1: Start-up, SAE Paper, No. 2000-01-2488.
26. J. Ku, L. Ottenstein, T. Kaya, et al., (2000) “Testing of a Loop Heat Pipe Subjected to Variable Accelerating Forces”, Part 2: Temperature Stability, SAE Paper, No. 2000-01-2489.
27. Y. Xie, J. Zhang, L. Xie, Y. Yu, H. Wu, H. Zhang,(2015)” Experimental investigation on the operating characteristics of a dual compensation chamber loop heat pipe subjected to acceleration field”, Appl. Therm. Eng. 81 (3) , 297–312.
28. K.N. Shukla, (2015) “Heat pipe for aerospace applications-an overview, J. Electron. Cooling Therm. Control 05, 1–14.
29. N. Putra, W.N. Septiadi, H. Rahman, R. Irwansyah, (2012) “Thermal performance of screen mesh wick heat pipes with nanofluids “, Exp. Therm. Fluid Sci. 40 , 10–17.
30. C.Y. Tsai, H.T. Chien, P.P. Ding, B. Chan, T.Y. Luh, P.H. Chen, (2004) “ Effect of structural character of gold nanoparticles in nanofluid on heat pipe thermal performance “, Mater Letters 58 ,1461–1465.
31. Y. Li, L.C. Lv, Z.H. Liu, Influence of nanofluids on the operation characteristics of small capillary pumped loop, Energy Convers. Manage. 51 (2010) 2312–2320.
32. C.W. Chan et al., (2015) “Heat utilization technologies: a critical review of heat pipes”, Renew. Sustain. Energy Rev. 50, 615–627.
33. C. Gerhart, D.F. Gluck, (1999) “Summary of operating characteristics of a dual compensation chamber loop heat pipe in gravity, in: Proceeding of the 11th International Heat Pipe Conference, Japan Association for Heat Pipes and Seikei University, Tokyo, Japan, September 1999.
34. D.F. Gluck, C. Gerhart, S. Stanley, (1999) Characterization of a high capacity, dual compensation chamber loop heat pipe, AIP Conf. Proc. 458 (1), 943–948.
35. Y. Xie, J. Zhang, L. Xie, Y. Yu, H. Wu, (2015)” Experimental investigation on the operating characteristics of a dual compensation chamber loop heat pipe subjected to acceleration field”, Appl. Therm. Eng. 81 , 297–312.